Green Synthesis of Silver and Gold Nanoparticles via Cactus Igneous Extract for Catalytic Reduction of Organic Dyes and Antibacterial Activity

Original Article

Mahmoud Baba Abdullahi[123], Dr Nik Noor Ashikin[1], Dr Idris Dauda Adamu[2], Dr Farhank Sabeer[1], and Abubakar Lawan Usman[1].

[1] School of Physics, Universiti Sains Malaysia, Pilau Pinang, Malaysia, [2]Physics Department, Bayero University, Kano, Nigeria, [3]Department of Physics, Aliko Dangote University of Science and Technology, Wudil, Kano, Nigeria.

Corresponding Author's Email: mahmoudbaba.phy@kustwudil.edu.ng; nnashikin@.usm.my

Submitted: 26 December, 2025 Final revision: 30 April, 2026 Accepted: 24 May 2026

ABSTRACT

The growing demand for sustainable nanomaterial synthesis has exposed significant limitations in conventional physical and chemical methods, including the use of toxic reagents, high energy consumption, and costly processing routes. In this study, a simple, rapid, and environmentally friendly green synthesis approach is reported for the fabrication of silver (AgNPs) and gold nanoparticles (AuNPs) using cactus plant extract as a natural reducing and stabilizing agent. The biosynthesized nanoparticles were systematically characterized using ultraviolet–visible (UV–Vis) spectroscopy, dynamic light scattering (DLS), selected area electron diffraction (SAED), energy-dispersive X-ray spectroscopy (EDX), X-ray diffraction (XRD), and atomic force microscopy (AFM). UV–Vis analysis confirmed nanoparticle formation through characteristic surface plasmon resonance peaks at 430–450 nm for AgNPs and 490–550 nm for AuNPs. DLS measurements revealed smaller hydrodynamic diameters for AgNPs (34.26–41.14 nm) compared to AuNPs (46.26–70.29 nm), while zeta potential values ranging from −13 to −21 mV indicated good colloidal stability. Furthermore, the synthesized nanoparticles exhibited notable catalytic efficiency in the degradation of methylene blue, demonstrating their potential for environmental remediation applications. The present work highlights the novelty and effectiveness of cactus-mediated green synthesis as a cost-effective, scalable, and sustainable route for producing functional metal nanoparticles with promising environmental applications.

Keywords: gold nanoparticles, green synthesis, cactus igneous, silver nanoparticles, catalytic activities

Online access: https://sjhrs.com.ng **DOI: https://doi.org/10.60787/sjhrs.vol1no1.11**

How to cite: Mamound et. al. Green Synthesis of Silver and Gold Nanoparticles via *Cactus Igneous* Extract for Catalytic Reduction. The Sub-Saharan Journal of Health & Radiation Sciences, 2026;1(1): 70 - 84

Introduction

The rapid advancement of nanotechnology has significantly increased the demand for sustainable and environmentally benign routes for nanoparticle synthesis. Conventional physical and chemical methods, although widely employed, suffer from major limitations such as the use of toxic reducing agents, high energy consumption, expensive instrumentation, and the generation of hazardous by-products, which restrict their large-scale and ecofriendly application (Baskar et al., 2023; Daphedar et al., 2023;)Among various green approaches, plant-mediated synthesis has emerged as an efficient, economical, and environmentally safe alternative for nanoparticle fabrication. Plant extracts contain diverse bioactive compounds including phenolics, flavonoids, terpenoids, alkaloids, and proteins that can act simultaneously as reducing, stabilizing, and capping agents (Rahman et al., 2022; Sharma et al., 2024).

Compared to conventional chemical methods that rely on synthetic reducing agents or polymeric stabilizers such as polyvinyl alcohol or polyols, plant-based synthesis offers superior biocompatibility, reduced toxicity, and simplified processing. Moreover, polymer-assisted synthesis often results in thick organic coatings on nanoparticles, which can hinder surface activity and negatively affect catalytic efficiency (Noruzi, 2015; Philip, 2008).

Metal nanoparticles, particularly silver (AgNPs) and gold nanoparticles (AuNPs), have attracted significant interest owing to their unique optical, catalytic, antimicrobial, and electronic properties. These nanomaterials have found extensive applications in catalysis, biosensing, drug delivery, environmental remediation, and wastewater treatment (Daphedar et al., 2023; Sarkar et al., 2023). However, many reported green synthesis studies suffer from drawbacks such as poor control over particle size, limited colloidal stability, prolonged synthesis time, and insufficient evaluation of catalytic performance. Additionally, several studies employ plant extracts with poorly characterized phytochemical profiles, limiting reproducibility and mechanistic understanding (Alizadeh & Ebrahimzadeh, 2025).

Environmental pollution caused by synthetic dyes has become a major global concern. Dyes such as methylene blue (MB),malacite green(MCGR) and 4-nitro are widely used in textile, pharmaceutical, and chemical industries and are highly toxic, non-biodegradable, and persistent in aquatic environments. Exposure to MB can cause serious health problems, including methemoglobinemia, cyanosis, and neurological disorders (Dheyab et al., 2025). Catalytic degradation using metal nanoparticles has emerged as an effective and environmentally sustainable strategy for dye removal, offering rapid degradation and conversion of toxic dyes into harmless by-products such as CO_2, H_2O, and inorganic ions.

Costus igneus (commonly known as the insulin plant) is a medicinal plant belonging to the Costaceae family and is rich in flavonoids, phenolic acids, alkaloids, and antioxidant compounds. It has been traditionally used for the treatment of diabetes and other metabolic disorders (Mahajan et al., 2018; Han et al., 2019). Despite its rich phytochemical profile and strong reducing potential, its application in nanoparticle synthesis remains largely unexplored. To the best of our knowledge, no previous study has reported the simultaneous green synthesis of both silver and gold nanoparticles using Costus igneus extract, nor evaluated their catalytic performance toward dye degradation.In this study, we present a rapid, inexpensive, and one-step green synthesis approach using extracts from cactus-type plants to fabricate stable and multifunctional silver (AgNPs) and gold nanoparticles (AuNPs). The synthesized nanoparticles were characterized using various spectroscopic and microscopic techniques to confirm their morphology, crystallinity, and surface chemistry. Furthermore, the biogenic nanoparticles are anticipated to exhibit excellent stability and promising bio-functional properties, highlighting their potential applications in antimicrobial, antioxidant, and cytotoxic studies

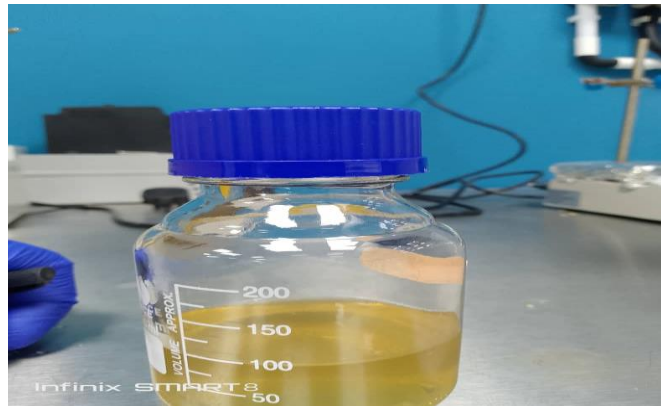

Plate I cactus igneous plant and cactus igneous plant Extarct

Material and Method

Chemicals and Reagents

Cactus Igneous was obtained from Pilau Pinang, Malaysia, and used as received. Hydrogen tetrachloroauric acid (III) trihydrate ($HAuCl_4 \cdot 3H_2O$), silver nitrate ($AgNO_3$).Methylene blue(MB), Malacite green 4 Nitro and sodium bought from Sigma Alderich Co (St Louis, MO U.S.A)

Preparation of Plant Extract

Cactus igneous Leaves were collected from the forest area of Gelugor, Pilau Pinang, Malaysia, and were cleaned with double-distilled water and shade-dried for a week at room temperature and further. Cactus leaves were crushed into pieces and stored for further study The plant leaves were washed several times with deionised water and dried at 25^{oC} in the oven, then separately.

The cleaned plant material was chopped into small pieces and boiled in distilled water (at 60–80$^{°C}$) for 15–30 minutes to extract bioactive compounds. The extract was filtered using Whatman filter paper to remove solid residues. The obtained filtrate was stored at 4°C for further use as a reducing and stabilising agent. For each synthesis, its extract is added once separately and another time together with 5 mL Cactus igneous to a vigorously stirred 1.0 mL aqueous solution of $HAuCl_4$ $3H_2O$ (7 mM), and stirring continued for 1 min. A slow reduction takes place and is complete in 1.5 h, as shown by the stable light violet colour of the solution, which gives colloid g1. To obtain colloids g_2, g_3 and g_4, the addition of the extract is varied as 10, 20 and 30 mL, respectively. It is found that reduction takes place rapidly with an increase in the addition of the extract, and colloid g_4 is obtained in 30 min. The colloids are found to be stable for 2 months.

Bio-Fabrication of CI-AgNPs and CI-AuNPs

The temperature, reaction time and concentration of CI extract and metal precursor for biosynthesis of AgNPs and AuNPs was optimized before this work. First, 1g of aqueous $AgNO_3$ (1 M) solution was put into the filtered extract of 1 mL CI (2 mg/mL) and incubated in water for 15 min at 80 ◦C. The color of suspensions went from yellow to dark orange. This suggested CI-AgNPs have synthesized. For synthesis of CI-AuNPs, 5 mL of the filtered CI extract (2 mg/mL) was added to 1 μL $HAuCl_4 \cdot 3H_2O$ (1 M) solution, following the processes of AgNPs synthesis. The change to violet color corroborated that CI-AuNPs had been synthesized.

Characterization. CI-AgNPs and CI-AuNPs

UV–visible spectra of NPs green-synthesized using CI were recorded using an Ultrospec 6300 pro UV-Vis spectrophotometer (Amersham Biosciences, Buckinghamshire, UK) in 300–800 nm at wavelengths. The particle size of the dispersions and zeta potential were analyzed by a Zetasizer, Nano-ZS90 (Malvern Panalytical, Malvern, UK).

A TALOS F200X (Thermo Scientific, Eugene, OR, USA) with EDX reveals HR-TEM images operating at 200 kV. The Ag and AuNPs were fixed onto a copper grid, Formvar/Carbon 200 Mesh(Electron Microscopy Sciences, Hatfield, PA, USA). X-ray diffractometer, X'Pert3 Powder (XRD Empyrean series 2, PANalytical, Almelo, Nederland), was used to reveal the structural information of NPs. The instrument was operated at 40 kV with 30 mA in current and Cu Kα radiation (1.540 Å) between 2θ◦from 20°c to 80°cfor analyzing the XRD pattern and crystal structure.

The SAED pattern of AgNPs reveals its crystalline nature (white dots in Fig.). The result of EDS gives a clear idea about the elements present in the nanoparticles. The EDS profile of phytocapped AgNPs is presented in Fig. 1. The strong signal of the Ag atoms indicates the crystalline property.

Catalytic Study of CI-AgNPs and CI-AuNPs

The catalytic potential for reduction of dyes was studied using the UV-Visible spectrophotometer with ice cold $NaBH_4$ at the room temperature. $NaBH_4$ solution was freshly prepared prior to the experiments. Then, 1mL aqueous solutions of MB (0.07 mM) and MCGR (0.05 mM) were added to 1 mL $NaBH_4$ (30 mM) and CI-AuNP (or CI-AgNP) solutions. Next, 2 mL of MG (0.1 mM) aqueous solution was mixed with 1 mL $NaBH_4$ (30 mM) and (AuNP or AgNP) solutions. CI-AgNP solution was added to the mixture at different volumes (150, 10, and 20 µL) of MB, MCGR, and 4-Nitro espectively. Meanwhile, the volume of the CI-AuNP solution added to the mixtures was 10 µL, except for the reduction of M, where it was 20 µL. The amount of green-synthesized AgNPs and AuNPs and the concentration of dyes and $NaBH_4$ for catalytic activities of CI-AgNPs and CI-AuNPs were optimized before these processes.(Zhang et al., 2021)

Dye degradation study

The degradation of organic dyes with sodium borohydride as a reducing agent has been studied using freshly prepared silver nanoparticles as catalysts at room temperature. Among the Organic dyes, methylene blue (MB), were used. All the solutions were prepared in distilled water and freshly prepared sodium borohydride solution was added to it. After that, silver nanoparticles were added, and the decomposition of specific dyes has been studied by observing the change in intensity of the absorption peak with time using a UV-vis spectrophotometer. All the degradation reactions are found to be fast, and 100% degradation has been achieved within a few minutes, as shown in

Result and Discussion

Green-synthesized cactus igneous silver nanoparticles (CI-AgNPs) and cactus igneous gold nanoparticles (CI-AuNPs) were successfully fabricated and characterized to investigate their potential (Figure 3). For CI-AgNPs, 1 mL of aqueous cactus igneous extract (2 mg/mL) was mixed with 1 µL of $AgNO_3$ solution (1 M). Within 15 minutes, the color of the extract changed to dark orange (Figure 3b), indicating the formation of nanoparticles through localized surface plasmon resonance (LSPR). The UV–Vis spectra, recorded between 300–800 nm, confirmed the synthesis of CI-AgNPs, showing a distinct LSPR absorption band at 422 nm.Similarly, CI-AuNPs were obtained by mixing 1 mL of aqueous cactus igneous extract (2 mg/mL) with 1 µL of $HAuCl_4 \cdot 3H_2O$ solution (1 M). After 15 minutes in a water bath, the colloidal solution turned purple (Figure 3c), suggesting successful nanoparticle formation. The UV–Vis spectra exhibited a strong LSPR band at 528 nm, characteristic of AuNPs.

Although earlier studies have reported the biofabrication of silver and gold nanoparticles using algae and plant extracts [Khan et al., 2022; Worakitjaroenphon et al., 2023], our findings highlight cactus igneous extract as a novel, eco-friendly reductant and stabilizing agent. For instance, Ramkumar et al. demonstrated the biosynthesis of silver nanoparticles with Enteromorpha compressa, yielding an LSPR peak at 421 nm, and further showed that red, green, and brown algae can also serve as effective reductants for nanoparticle synthesis.

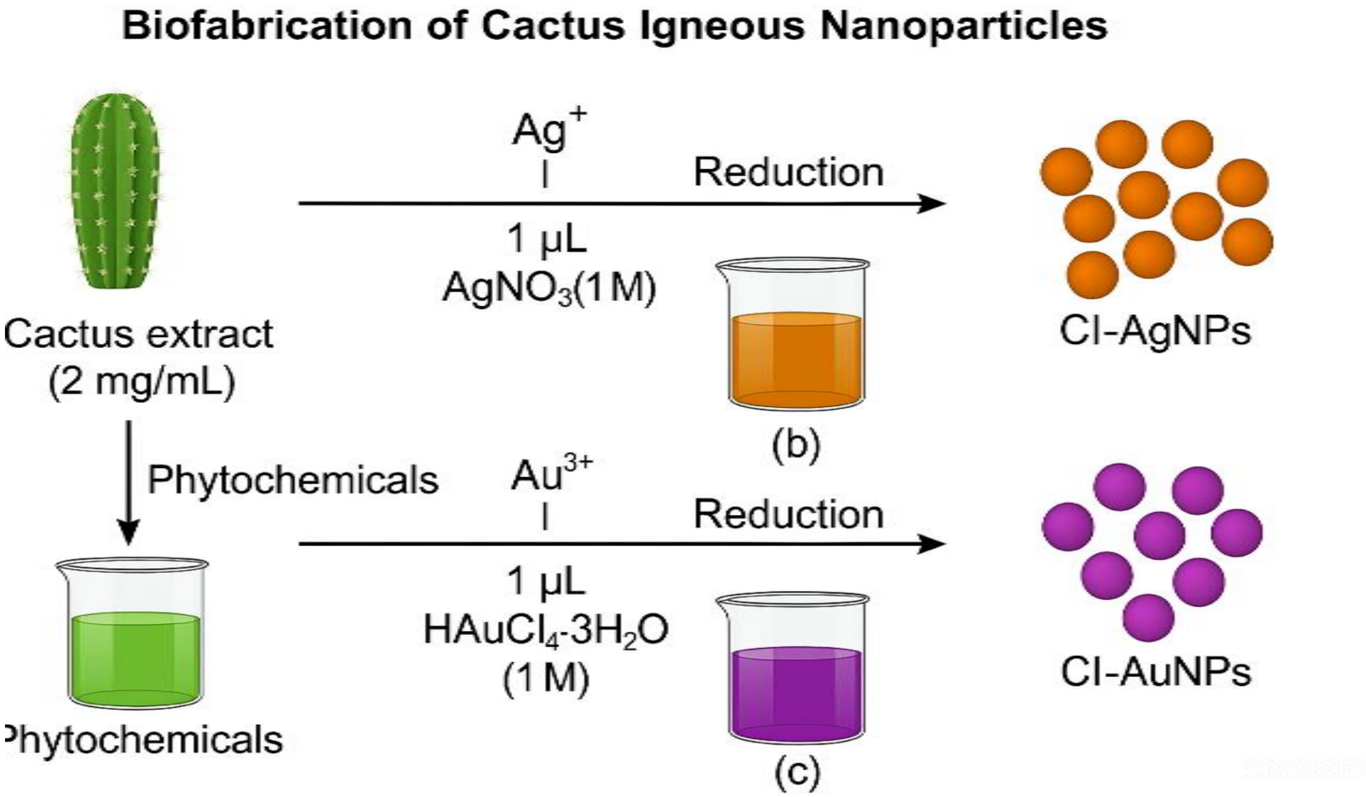

Figure 2.0 schematic meachanism of formation silver and gold nanoparticles

UV–visible analysis

The key approach for confirming the production of Cactus igneous AuNPs and AgNPs was UV–Vis analysis. The solution changed colour from light yellow to purple due to the synthesis of Cactus igneous AuNPs and from colourless to ruby brown for AgNPs. Fig. 3 depicts the UV–vis absorption spectra as a function of time. The Cactus igneous AuNPs were produced in 120 min, and the NPs development was tracked and retrieved every 30 min. At nanometre dimensions, the electron cloud can oscillate on the particle surface and absorb electromagnetic radiation at a particular energy. This resonance, known as surface plasmon resonance (SPR) or plasmon absorbance of nanoparticles, is a consequence of their small size, but it can be influenced by numerous factors; in particular, solvent and surface functionalization are important contributors to the exact frequency and intensity of the band. This dependence on surface effects makes the surface plasmon an ideal monitor of the absorption, which allows nanoparticle assembly to be used as a sensing device. (Hamelian et al., 2018).

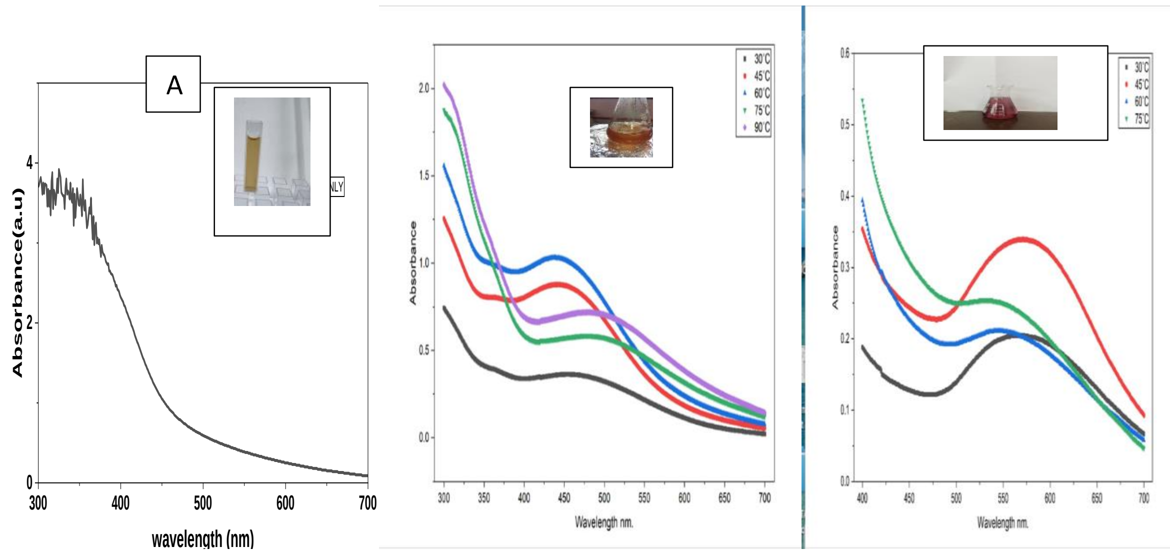

Fig 3.Ultraviolet visible (UV-VIS) Spectrar of (a) extract (b)CI-AgNPs(silver nanoparticles) and (c)CI-AuNPs(gold nanoparticles) at different temperature

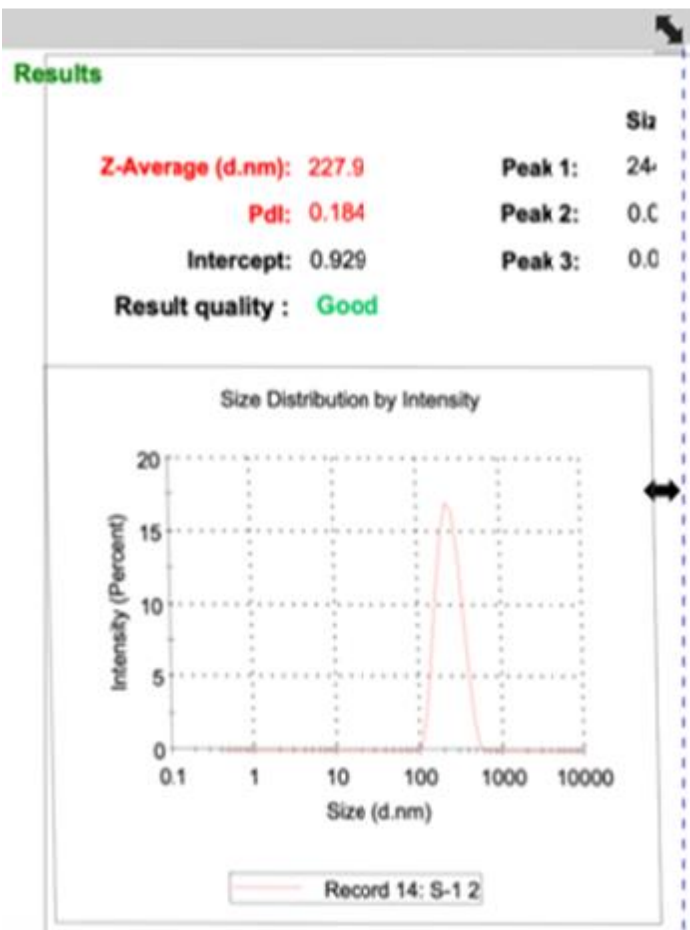

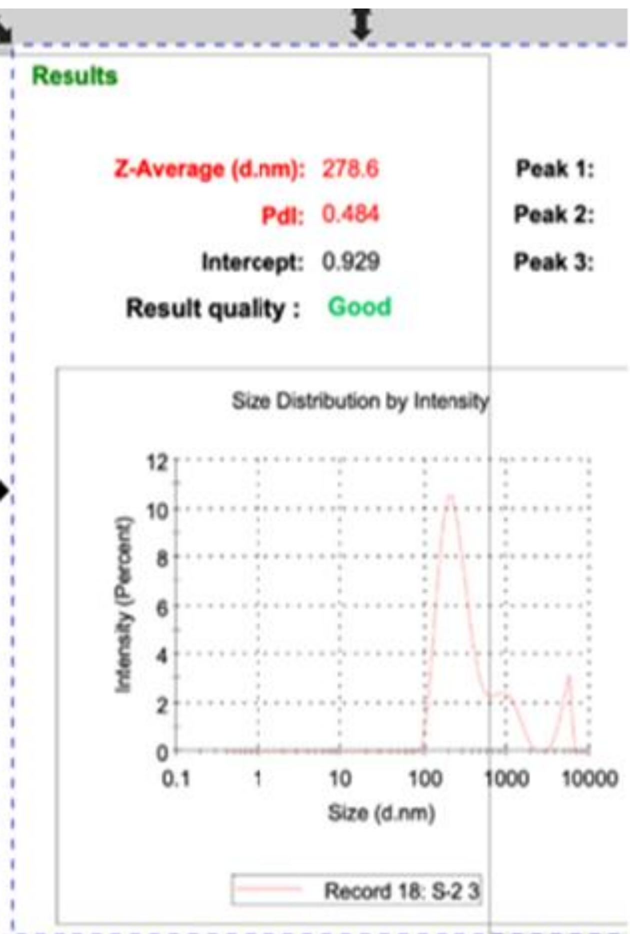

Figure 4 dynamic light scattering(DLS)Showing the collaidal size of zeta potentialsof (a)

Figure 4 zeta potential cactus igneous gold and silver nanoparticles

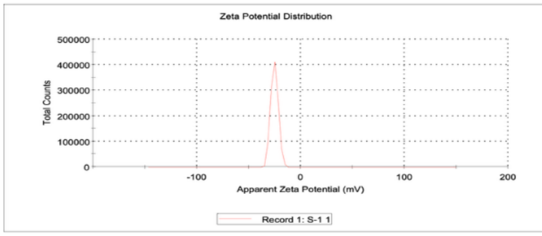

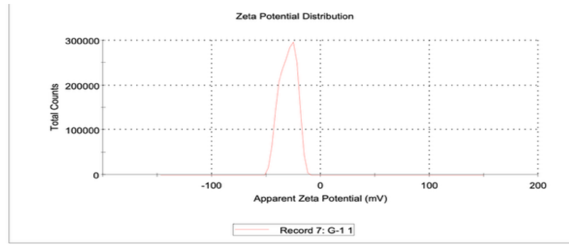

Figure5a. Zeta potential of silver nanoparticles

Figure 5b Dynamic light scattering (DLS)showing the colloidal size and zeta potential of (a)CI-AgNPs and (b)CI-AuNPs nanoparticles. The results of the UV–visible analysis are in agreement with those of earlier studies. (Azadmanesh et al., 2025; Stalin et al., 2025) Figure uv-vis of malacite green only

Dynamic Light Scattering (DLS) and Zeta potential

DLS is an analytical technique that is used for routine measurement of the size of NPs. With the user-friendly operation and low cost of this technique in comparison to other sophisticated instruments, DLS has become the popular technique for size measurement of any metallic NPs, including AuNPs and AgNPs.DLS analysis demonstrate a Z-average of 227.9nm with an acceptable polydispersity index(0.184) for gold nanoparticles whereas Z-average of 278.6nm andpoly dispersity index 0.484 for silver nano particles. A polydispersity index (PI) sows an acceptable range of hydrodynamic size particle. A higher Zaverage compared to solid phase crystalline size indicates that the particle tended to agglomerate in water. The agglomeration was relatively hight and the particle diameter was more then 2 times then SEM

Zeta Potential Analysis

Zeta potential can be considered an important tool to measure the physical stability of nanoparticles The zeta potential of a sample is most often used as an indicator of dispersion stability. Large zeta potentials predict a more stable dispersion. Fast and accurate measurement of the zeta potential with the nanoparticle SZ-100V2 can enhance understanding of aggregation and flocculation in samples and speed up the process of developing stable formulations, be they dispersions, emulsions, or suspensions.

The figure 4 shows the DLS analysis to find out the hydrodynamic distribution of size for CI-AgNPs and CI-AuNPs. The average size of CI-AgNPs that DLS measured was 120.0 ±3.85 nm and that of CI-AuNPs was 17.47 ±0.13 nm at 25°C. The polydispersity index was 0.397 and 0.744, respectively.The zeta potential measurements that identify the stability of nanoparticles were −25.3 and −30.1 mV, respectively, as shown in Figure. These large negative values of zeta potential indicated a good stability of the colloidal solutions of CI-AgNP and -AuNP.

SEM with EDX

Scanning electron microscopy (SEM) is used for morphological characterization at the nanometre to micrometer scale [Worakitjaroenphon et al., 2023]. SEM analysis shows uniformly distributed silver and gold nanoparticles, indicating the stabilization of nanoparticles by capping agents. The silver and gold nanoparticles were spherical in shape with particle size range from 19.62 to 31.3 nm. The larger gold particles may be due to the aggregation of the smaller ones, according to the SEM measurements (Fig7a). In EDAX strong signals were observed from the gold atoms in the nanoparticles and weaker signals for carbon, oxygen,potassium and chloride were provenients from biomolecules of Cactus igneous (Fig7) (Fig. 7b). Elemental gold can be seen in the graph

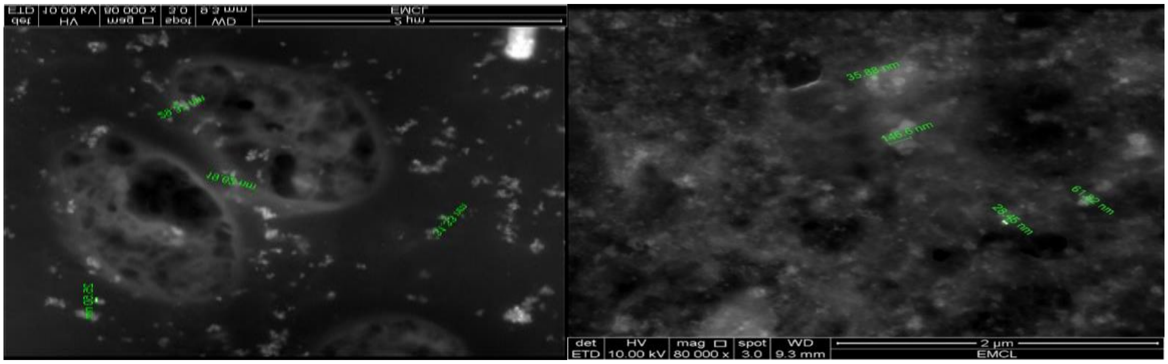
det HV mag spot WD 2 µm
ETD 10.00 kV 80 000 x 3.0 9.3 mm EMCL

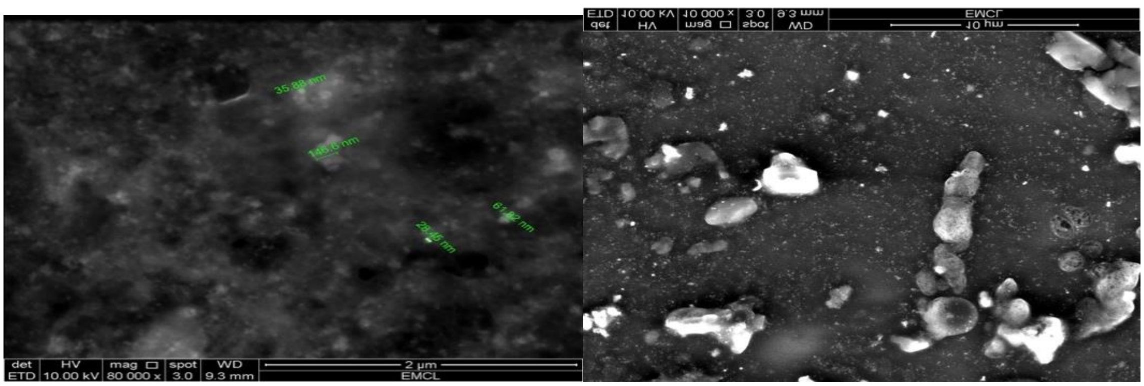
det HV mag spot WD 2 µm
ETD 10.00 kV 80 000 x 3.0 9.3 mm EMCL

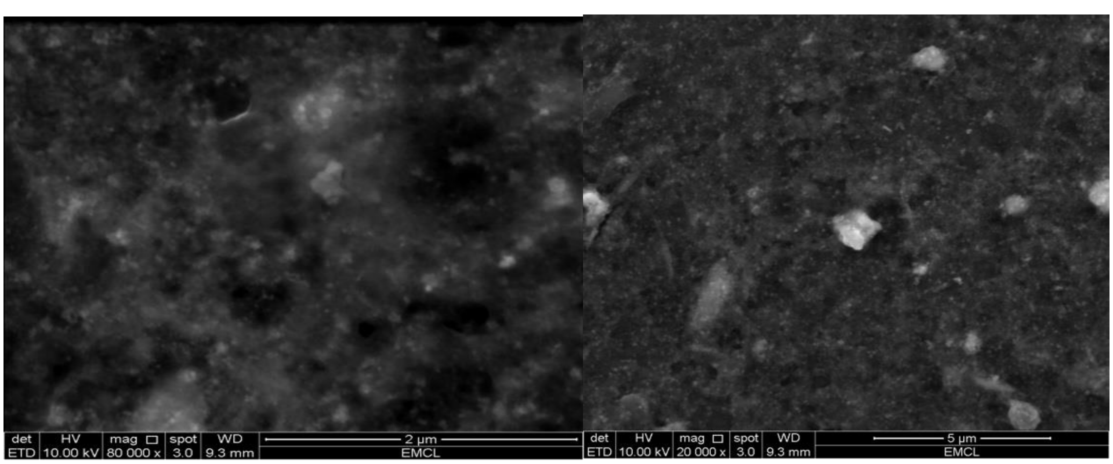
det HV mag spot WD 2 µm
ETD 10.00 kV 80 000 x 3.0 9.3 mm EMCL
det HV mag spot WD 5 µm
ETD 10.00 kV 20 000 x 3.0 9.3 mm EMCL

figure6 different magnification of biosynthesized AuNPs and AgNPs

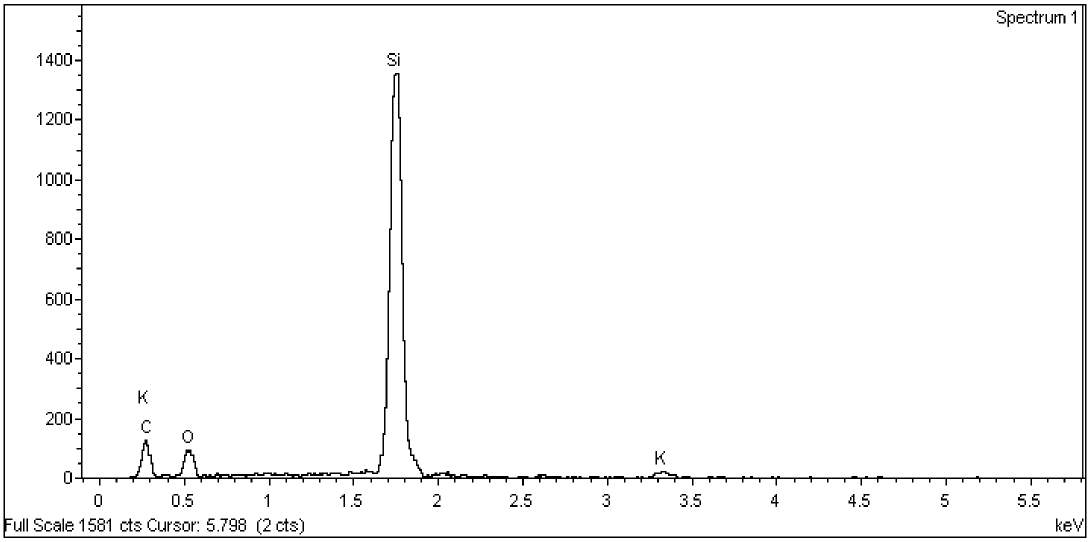

Figure7 EDX Pattern of gold nanoparticle

The SEM pattern of AgNPs reveals its crystalline nature (white dots in Fig.6). The result of EDS gives a clear idea about the elements present in the nanoparticles. The EDS profile of phytocapped AgNPs is presented in Fig7. . The strong signal of the Ag atoms indicates the crystalline property. The presence of O peaks along with the Ag signals suggests that the AgNPs are capped by phytoconstituents through oxygen atoms. The Cu peak comes from the TEM grid. The size of the synthesized AgNPs are approximately 25 nm.

X-RD

X-Ray Diffraction Analysis

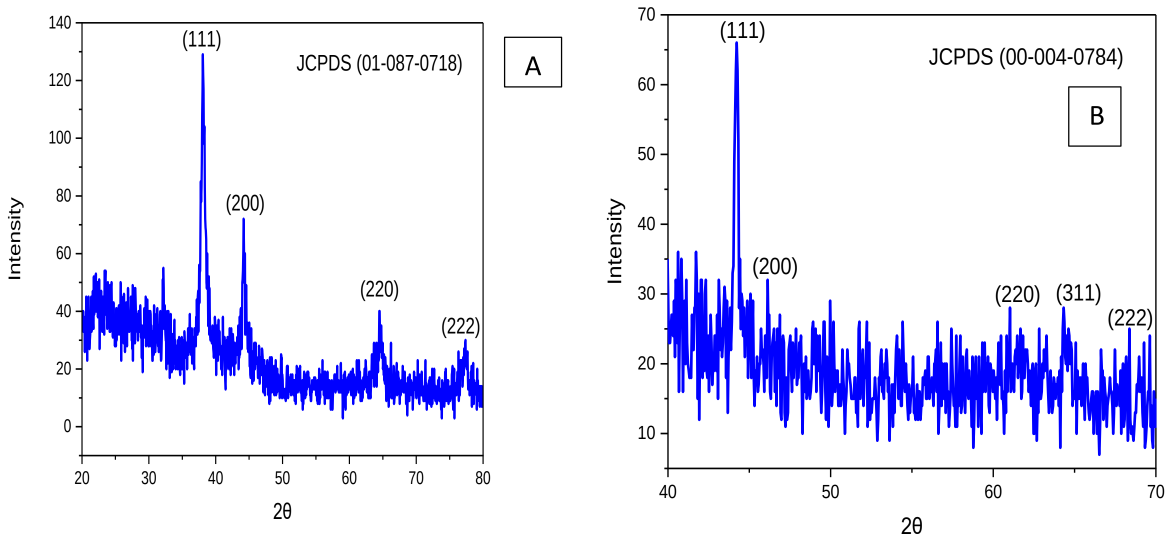

Fig 8 X- ray diffraction (XRD) reflection spectrar (a)CI-AgNPs and (b)CI-AuNPs

XRD is primarily used to identify crystallographic phases and characterize the crystalline nature at room temperature of CI-AuNPs.The figure displayed that the X-RD pattern of AgNPs and AuNPs .The diffraction peak were detected in the 2θ angles in the range of 20-80^0 which can be indexed (1, 1, 1,), (2, 0, 0), (2 ,2, 0) and (3 1 1),As a result it confirms the synthesized AgNPs and AuNPs planes have face-centered-cubic (F,C,C,) crystalline structure geometry of AgNPs, which is in agreement with the JCPDS file No. 00-004-0784 for gold. The ratio between the intensities of (1, 1, 1,) and (2 0 0) diffraction peaks is relatively higher than the usual values which indicate that the experimental system has AgNPs oriented in (1 1 1) plane .This result indicates that synthesized nanoparticles are composed of crystalline silver and gold. Some of the minor peaks are presented due to the presence of organic moieties or biomolecules derived from plant extract The average crystalline structure size of synthesized AgNPs and AuNPs was estimated by Scherrer's formula

$$D = \frac{k\lambda}{\beta cos\theta}$$

Where D is the mean crystall size K is constant(0.94). λ is the wavelength, theta is the Bragg's angle, β is the full with half maximum of the diffraction peak.

This result was cofirmed with calculted mean diameter from

AFM study of nanoparticle

CI-AgNP and CI-AuNPs were characterize by AFM and imaging result are illustrated in the figure 9 by evaluating the NPs' height. The NPs were identified as bright pixels (yellow colored areas) within the topography maps. For example, the left images in panels (a) and (b) of fig 9 show the raw AFM topography. Next to them are the images in which the color of the pixels identified as NPs represents the value of the assessed NP diameter. The exact diameter values are given in the graphs at the right end of the corresponding panels. For the particular case illustrated in fig3, the diameter of Ag@CI NPs varies between 9 nm and 26 nm (see panel (a)), whereas the diameter of Au@CI NPs varies between 13 nm and 34 nm (see panel (b)).

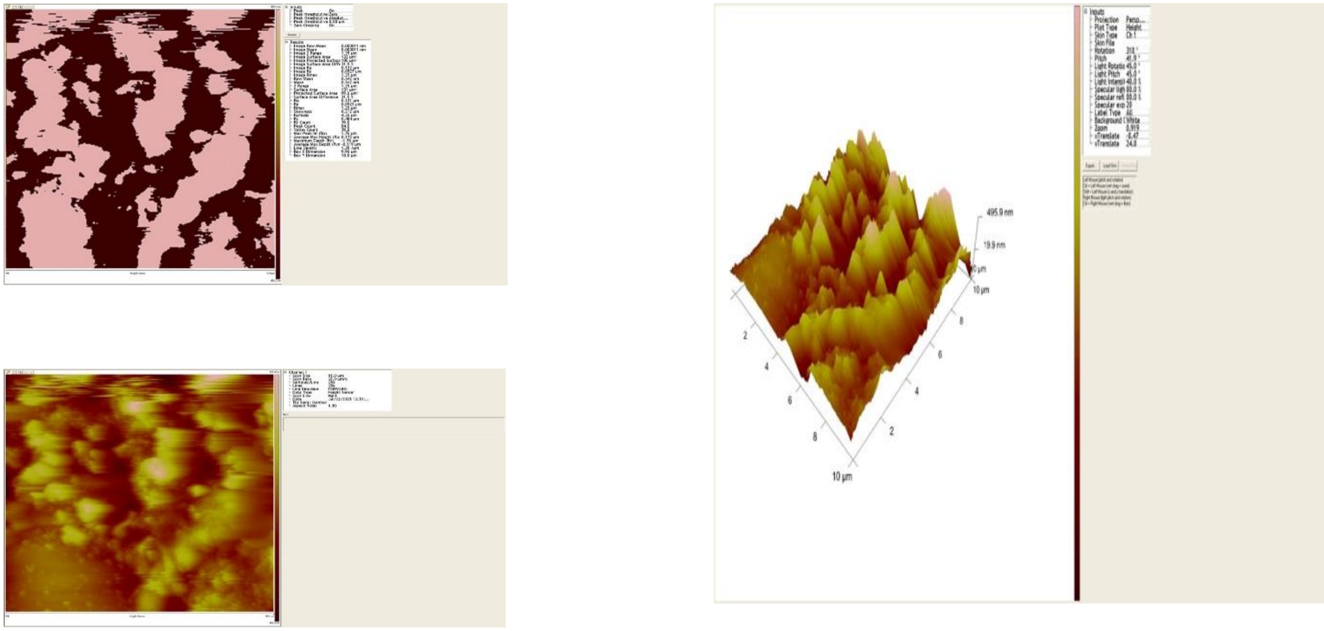

Fig 9 atomic force microscopic for the synthesized

The average NPs height was determined by analyzing a series of AFM topography maps (10 maps per NP type, either Ag@CI NPs orAu@CI NPs).Fig shows the Ag@CI- NPs and Au@CI NPs diameter distribution, with the average values given in

Antibacterial activity

The antibacterial activity of CI-AuNPs and CI-AgNPs against selected bacterial strains were displayed in Fig10 . The obtainede result indicates that the CI-AgNPs and CI-AuNPs were harmful to all the tested bacterial strains at various doses. Among the bacterial strain examined, CI-AgNPs and CI-AuNPs exhibited the strongest inhibitory activity against 12.67 ±0.24, and 11.42 ± 0.58 mm,at the highest concentration (40 L) Table 1. When metal ions in solution come into contact with a bacterial cell, they become generally dispersed in the environment around the bacterial cell, with no specific localization. NPs that engage with the bacterial cell wall, on the other hand, form a focused source of ions that constantly release ions, increasing cell toxicity. Our results showed that the CI-AgNPs and AuNPs have a better antibacterial effect against bacteria. This could be because bacteria has strong cell wall, whereas gram-negative bacteria has thin cell wall so the CI-AgNPs and AuNPs easily penetrate to the cell membrane of the gram-negative bacteria and causes damages to the cell The antibacterial property of silver and gold NPs was achieved in two processes. They inhibited the metabolic process by changing the membrane potential and lowering adenosine triphosphate (ATP) synthase activity. Second, they rejected the ribosome's subunit for RNA binding, effectively dismantling its biological process. They were also found to be less harmful to mammalian cells. Silver and Gold nanoparticles in various dimensions and shapes are the most widely investigated nanomaterials for antibacterial and anti-biofilm applications, according to a recent literature review. Electronic effects are produced by Silver and gold NPs with a small size and increased surface area, which are advantageous for increasing the surface reactivity of NPs. Furthermore, the high surface area percentage immediately interacted with the bacterium to a large amount, resulting in improved bacteria interaction. The antibacterial activity of the NPs with large surface area was considerably increased by these two critical features. Previous research has shown that gold nanoparticles play an important role in drug delivery and can be used to combat a wide range of pathogenic bacteria due to their effective antibacterial properties . The findings suggest that CI-AuNPs and CI-AgNPs may be a useful tool for antibacterial drug for now and in the future.

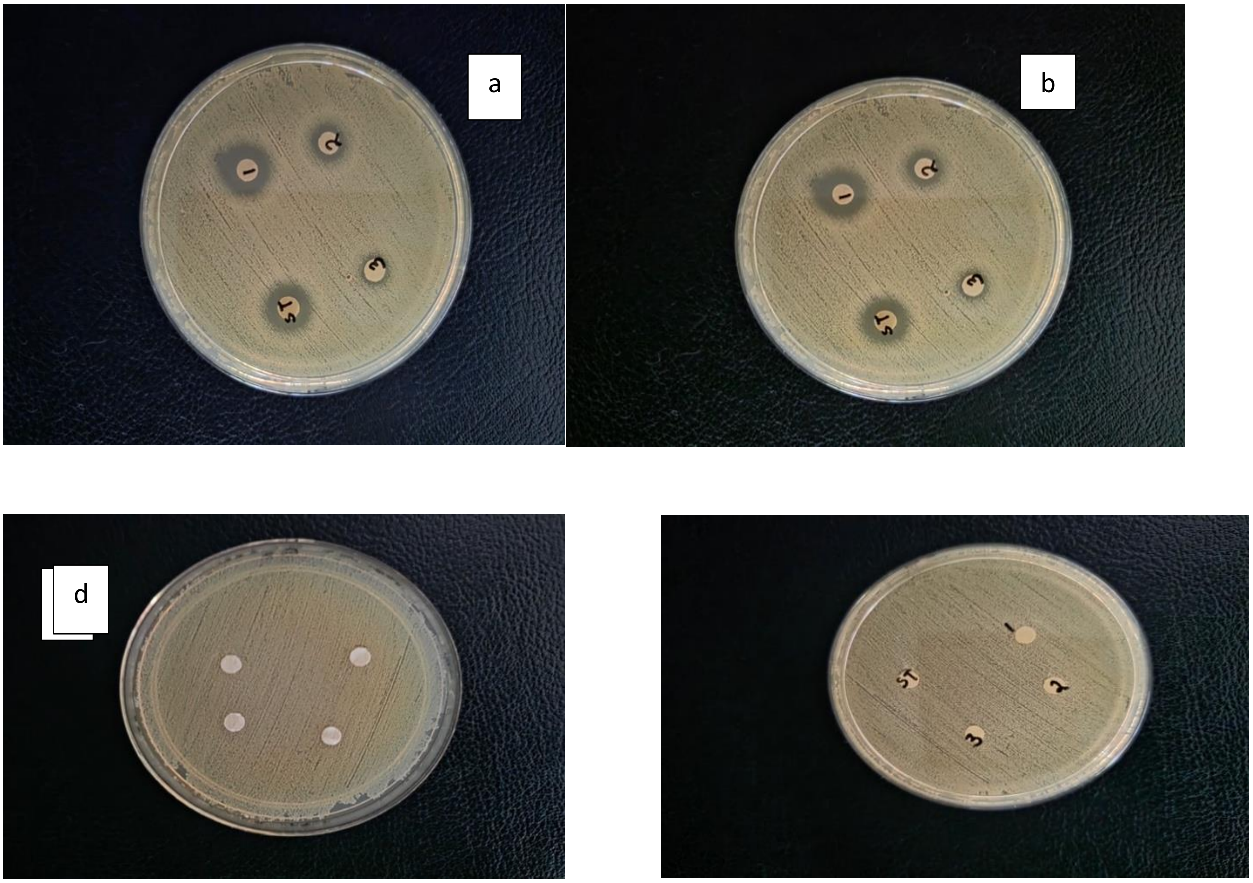

Figure10 Antibacterial activities of cactus igneous extract and greener synthesized AgNPs (CI-AgNPs) against bacteriADRES

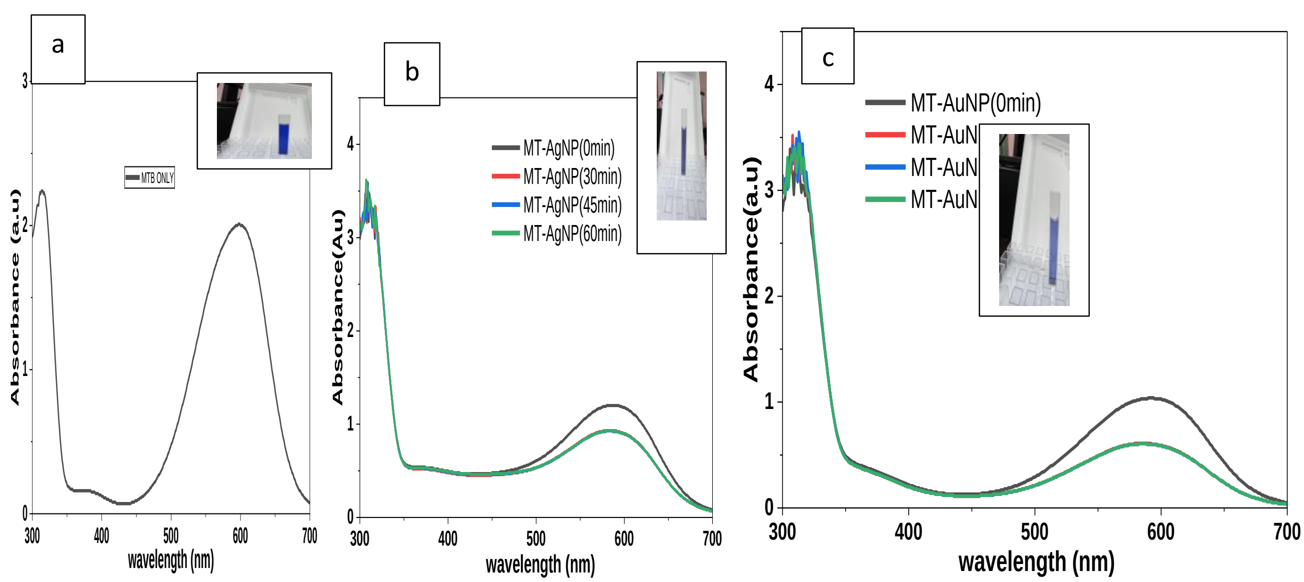

Fig 11 uv -vis spectrar of methylene blue dye reduction in the presence of (NaBH4 (b) CI-AgNPs (c)CI-AuNPs

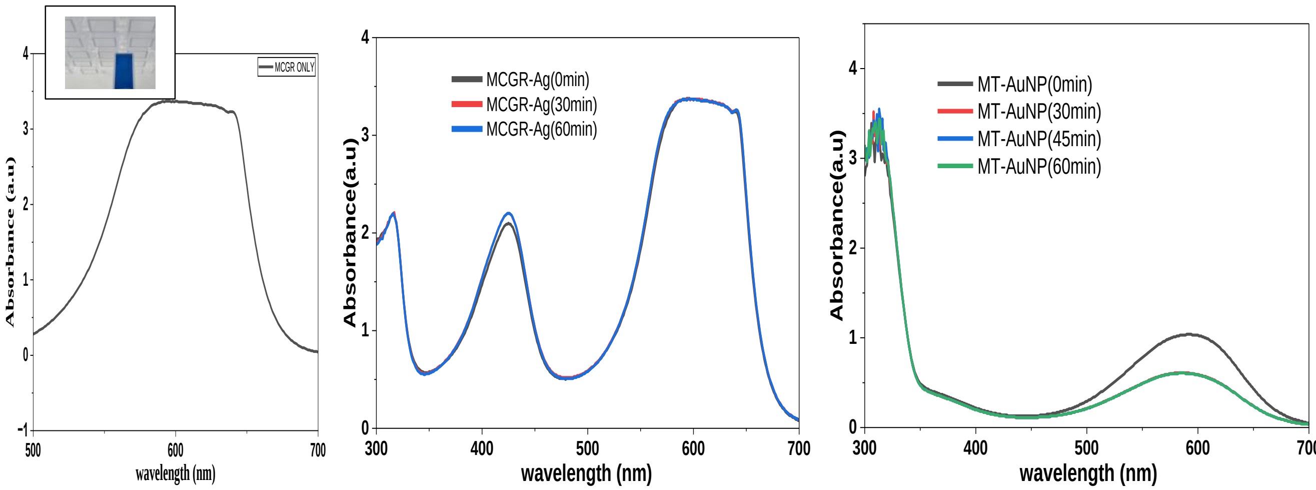

Fig 12 uv -vis spectrar of methylene Green dye reduction in the presence of(a) extract (b) CI-AgNPs (c)CI-AuNPs

Conclusion

In this work,the fabrication of AgNPs and AuNPs by Cactus igneous via a green method is an economic and eco-friendly method, which could be helpful to human health and environmental subjects.The UV–Vis spectroscopy and EDX analysis substantiated the synthesis of CI-NPs. The size, zeta potential and morphology were revealed by DLS and HR-TEM. The XRD and SAED patterns confirmed that CI-AgNPs and CI-AuNPs were crystalline, FCC in structure. These green-synthesised NPs have excellent performance of catalytic activities for reducing MB, by $NaBH_4$ at room temperature. From the kinetic studies, the results suggested that the reduction of dyes followed a pseudo-first order and the rate constants (k) could be obtained. In conclusion, algae-based synthesized NPs have excellent catalytic activity and reactivity as cheap, desirable and environmentally safe nanocatalysts for the effective decomposition.

REFERENCES

1. Alizadeh, S. R., & Ebrahimzadeh, M. A. (2025). Catalytic degradation of organic dyes using Allium paradoxum extract mediated gold nanoparticles. *International Journal of Environmental Science and Technology*, *22*(4), 2659–2672. https://doi.org/10.1007/s13762-024-05971-4

2. Azadmanesh, M., Noorbakhsh, M. F., Nazifi, S., & Faraji, M. (2025). Green Synthesis and Characterization of Silver and Gold Nanoparticles Using Echinophora platyloba Extract and Evaluation of Their Anti-Inflammatory and Antioxidant Properties. *Oxidative Medicine and Cellular Longevity*, *2025*(1). https://doi.org/10.1155/omcl/4421985

3. Baskar, G., Palaniyandi, T., Viswanathan, S., Rahaman Abdul Wahab, M., Surendran, H., Ravi, M., Kumar Rajendran, B., Govindasamy, G., Sivaji, A., & Kaliamoorthy, S. (2023). Pharmacological effect of gold nanoparticles from red algae Halymenia venusta on A549 cell line. *Inorganic Chemistry Communications*, *155*. https://doi.org/10.1016/j.inoche.2023.111005

4. Daphedar, A. B., Kakkalameli, S., Faniband, B., Bilal, M., Bhargava, R. N., Ferreira, L. F. R., Rahdar, A., Gurumurthy, D. M., & Mulla, S. I. (2023). Decolorization of various dyes by microorganisms and green-synthesized nanoparticles: current and future perspective. In *Environmental Science and Pollution Research* (Vol. 30, Issue 60, pp. 124638–124653). Springer. https://doi.org/10.1007/s11356-022-21196-9

5.

6. 5. Dheyab, M. A., Aziz, A. A., Nowfal, S. H., Braim, F. S., Abdullah, W., Kasasbeh, W. H., Jameel, M. S., Alanezi, S. T., Alrosan, M., & Oladzadabbasabadi, N. (2025). Sustainable green synthesis of silver nanoparticles for safer biomedical application. In *Journal of Environmental Chemical Engineering* (Vol. 13, Issue 2). Elsevier Ltd. https://doi.org/10.1016/j.jece.2025.115998

7.

8. 6. Hajam, Y. A., Kumar, R., Reshi, M. S., Rawat, D. S., AlAsmari, A. F., Ali, N., Ali, Y. S. M., & Ishtikhar, M. (2022). Administration of Costus igneus Nak leaf extract improves diabetic-induced impairment in hepatorenal functions in male albino rats. *Journal of King Saud University - Science*, *34*(4). https://doi.org/10.1016/j.jksus.2022.101911

9. 7. Jadoun, S., Arif, R., Jangid, N. K., & Meena, R. K. (2021). Green synthesis of nanoparticles using plant extracts: a review. In *Environmental Chemistry Letters* (Vol. 19, Issue 1, pp. 355–374). Springer Science and Business Media Deutschland GmbH. https://doi.org/10.1007/s10311-020-01074-x

8. Khan, F., Shahid, A., Zhu, H., Wang, N., Javed, M. R., Ahmad, N., Xu, J., Alam, M. A., & Mehmood, M. A. (2022). Prospects of algae-based green synthesis of nanoparticles for environmental applications. *Chemosphere*, *293*. https://doi.org/10.1016/j.chemosphere.2022.133571

9. Noruzi, M. (2015). Biosynthesis of gold nanoparticles using plant extracts. In *Bioprocess and biosystems engineering* (Vol. 38, Issue 1, pp. 1–14). https://doi.org/10.1007/s00449-014-1251-0

10. Patil, T. P., Vibhute, A. A., Patil, S. L., Dongale, T. D., & Tiwari, A. P. (2023). Green synthesis of gold nanoparticles via Capsicum annum fruit extract: Characterization, antiangiogenic, antioxidant and anti-inflammatory activities. *Applied Surface Science Advances*, *13*. doi.org/10.1016/j.apsadv.2023.100372
11. Philip, D. (2008). Synthesis and spectroscopic characterization of gold nanoparticles. *Spectrochimica Acta - Part A: Molecular and Biomolecular Spectroscopy*, *71*(1), 80–85. https://doi.org/10.1016/j.saa.2007.11.012

12. Rahman, S., Al-Harbi, F. F., Ajmal, M., Naseem, A., Farooqi, Z. H., & Siddiq, M. (2022). Engineering of micron-sized spherical anionic microgel fabricated with silver nanoparticles with antimicrobial and catalytic potential. *Journal of Materials Science*, *57*(12), 6763–6779. https://doi.org/10.1007/s10853-022-07042-w

13. Sarkar, P., Paul, S. K., Sahu, K., Mandal, S., Islam, Q. A., & Chakrabarty, R. (2023). A Greener Synthesis of Silver Nanoparticles Using Tea Leaf and Aloe Vera Leaf Extract for Catalytic Organic Dye Degradation Application. *ChemistrySelect*, *8*(28). https://doi.org/10.1002/slct.202301906

14. Sharma, A., Sunny, S., Arulraj, J., & Hegde, G. (2024). Exploring the efficiency of green synthesized silver nanoparticles as photocatalysts for organic dye degradation: unveiling key insights. In *Nano Express* (Vol. 5, Issue 2). Institute of Physics. https://doi.org/10.1088/2632959X/ad4d09

15. Stalin, N., Ramar, D., Esakkirajan, M., ArunPrasanna, V., Arumugam, A., & Gopinath, K. (2025). Green synthesis-driven gold nanoparticles using Lilium wallichianum leaf extract for biomedical applications. *Inorganic Chemistry Communications*, *178*. https://doi.org/10.1016/j.inoche.2025.114507

16. Worakitjaroenphon, S., Shanmugam, P., Boonyuen, S., Smith, S. M., & Chookamnerd, K. (2023). Green synthesis of silver and gold nanoparticles using Oroxylum indicum plant extract for catalytic and antimicrobial activity. *Biomass Conversion and Biorefinery*. https://doi.org/10.1007/s13399-023-04734-4

17. Yadav, M., Yadav, P., Yadav, J. P., & Kataria, S. K. (2024). Novel derivatives of Costus igneus towards potentiality against diabetes mellitus receptors: ADME/Tox profiling, Computational Docking, and Molecular Dynamics Simulation study. *Journal of Taibah University for Science*, *18*(1). doi.org/10.1080/16583655.2024.2370107

18. Alizadeh, S. R., & Ebrahimzadeh, M. A. (2025). Catalytic degradation of organic dyes using Allium paradoxum extract mediated gold nanoparticles. *International Journal of Environmental Science and Technology*, *22*(4), 2659–2672. https://doi.org/10.1007/s13762-024-05971-4

19. Azadmanesh, M., Noorbakhsh, M. F., Nazifi, S., & Faraji, M. (2025). Green Synthesis and Characterization of Silver and Gold Nanoparticles Using Echinophora platyloba Extract and Evaluation of Their Anti-Inflammatory and Antioxidant Properties. *Oxidative Medicine and*

Cellular Longevity, *2025*(1). https://doi.org/10.1155/omcl/4421985

20. Baskar, G., Palaniyandi, T., Viswanathan, S., Rahaman Abdul Wahab, M., Surendran, H., Ravi, M., Kumar Rajendran, B., Govindasamy, G., Sivaji, A., & Kaliamoorthy, S. (2023). Pharmacological effect of gold nanoparticles from red algae Halymenia venusta on A549 cell line. *Inorganic Chemistry Communications*, *155*. https://doi.org/10.1016/j.inoche.2023.111005

21. Daphedar, A. B., Kakkalameli, S., Faniband, B., Bilal, M., Bhargava, R. N., Ferreira, L. F. R., Rahdar, A., Gurumurthy, D. M., & Mulla, S. I. (2023). Decolorization of various dyes by microorganisms and green-synthesized nanoparticles: current and future perspective. In *Environmental Science and Pollution Research* (Vol. 30, Issue 60, pp. 124638–124653). Springer. https://doi.org/10.1007/s11356-022-21196-9

22. Dheyab, M. A., Aziz, A. A., Nowfal, S. H., Braim, F. S., Abdullah, W., Kasasbeh, W. H., Jameel, M. S., Alanezi, S. T., Alrosan, M., & Oladzadabbasabadi, N. (2025). Sustainable green synthesis of silver nanoparticles for safer biomedical application. In *Journal of Environmental Chemical Engineering* (Vol. 13, Issue 2). Elsevier Ltd. https://doi.org/10.1016/j.jece.2025.115998